Structural characterization of the hard fullerite phase obtained at 13 GPa and 830 K

A. V. Talyzin,[1,*] F. Langenhorst,[2,3] N. Dubrovinskaia,[2] S. Dub,[4] and L. S. Dubrovinsky[2]
[1]*Department of Physics, Umeå University, 901 87 Umeå, Sweden*
[2]*Bayerisches Geoinstitut, Universität Bayreuth, D-95440 Bayreuth, Germany*
[3]*Friedrich-Schiller-Universität Jena, Institut für Geowissenschaften, Burgweg 11, D-07749 Jena, Germany*
[4]*Institute for Superhard Materials, Kiev, 04074, Ukraine*
(Received 18 March 2004; revised manuscript received 13 October 2004; published 24 March 2005)

A detailed characterization of two samples synthesized at 13 GPa and 830 K with heating times of 20 min and 1 h, respectively, was performed using x-ray diffraction (XRD), Raman spectroscopy, and high-resolution transmission electron microscopy (HRTEM). The sample heated for 20 min was amorphous and exhibited a high hardness of 45 GPa, while the second sample appeared to be softer and crystalline. A slightly distorted fcc cubic packing was found by XRD and HRTEM. Both samples are proved to consist of unbroken C_{60} molecules. The crystalline sample was also studied by *in situ* XRD during compression up to 26 GPa using synchrotron radiation. The bulk modulus value of 217 GPa obtained from compression experiments is in good agreement with the measured hardness of the sample (37 GPa). The Raman spectroscopy shows an unusual combination of features: some additional peaks compared to untreated C_{60} and no shift for the $A_g(2)$ mode.

DOI: 10.1103/PhysRevB.71.115424 PACS number(s): 61.48.+c, 61.10.Nz, 68.37.Lp, 62.50.+p

I. INTRODUCTION

Fullerene C_{60} undergoes polymerization at high-pressure high-temperature conditions (HPHT). Below 9 GPa and 900 K several kinds of one (1D)- and two-dimensional (2D) polymeric phases have been obtained: orthorhombic, tetragonal, and rhombohedral. At the moment, 1D and 2D polymeric phases are well characterized by different techniques, including Raman spectroscopy, x-ray diffraction (XRD), etc.[1–7] Most of these studies were performed *ex situ* after cooling the sample and release of pressure. Only recently, some *in situ* studies of polymerization at HPHT conditions were performed.[8–13]

Three-dimensionally (3D) polymerized "superhard" fullerites have been claimed to exist at pressures above 12–13 GPa and temperatures above 800 K.[14–25] The structural characterization of these phases is very difficult, but their extremely high hardness has attracted a lot of attention. Several structural models have been proposed for these superhard phases, including different hypothetical kinds of bonding between C_{60} molecules but none of them is well proven.[23–26] The problem with characterization of these superhard phases is that they are either completely amorphous or exhibit very few lines in XRD, which allows a quite ambiguous interpretation. Raman spectra of these phases are also typically almost featureless and have been interpreted by some researchers as "collapsed" fullerite with only fragments of C_{60} cages remaining. Similar Raman spectra have also been obtained for C_{60} samples pressurized at room temperature above 25 GPa.[27–30] One of the main problems in studies of the superhard phases is poor reproducibility. The samples obtained by different groups at the same pressure-temperature conditions showed different properties. One of the most interesting points in the *P-T* diagram of C_{60} is at about 13 GPa and 830 K. Samples obtained at these conditions have been reported harder than diamond by Blank *et al.*,[14–19] but softer than diamond by Brazkin *et al.*[20,21] They appeared even softer in our previous studies performed using diamond anvil cells (DACs). Strong divergence of the results is most probably explained by different experimental techniques used to obtain samples.

Only recently, it became clear that not only pressure and temperature, but also some other experimental parameters, such as heating time, stress, and *P-T* history can be directly connected to physical properties of synthesized samples. For example, studies in DACs have shown that pressure variations during the heating can be very strong, and therefore special design of DACs is required to maintain constant pressure.[11–13] This observation is rather important because in most of the studies that were conducted *ex situ*, the *P-T* history of samples remains unknown. It is especially true for experiments by Blank *et al.*,[14–19] because they used very short heating time (1 min) without control over pressure variation during the heating. It is also clear that particularities of the experimental method applied by Blank *et al.* result in a strong shear deformation of their samples. The deformation has been so strong that the samples studied by Marcus *et al.* exhibited ellipse-like XRD patterns instead of normal Debye-Scherrer rings.[22] Other studies conducted at the same pressure-temperature region without strong stress showed no elliptical XRD patterns.[11–13] It has also been shown that strong stress favors polymerization. The superhard phase can be obtained even at room temperature when strong shear deformation is combined with high pressure.[15] Finally, it has been found that the hardness of the samples treated at some certain pressure-temperature depends on heating time. The studies by Horikawa *et al.* showed that hardness dependence on heating time is nonlinear and goes through a maximum at 10–60 min (15–12 GPa, respectively), and that longer heating produces softer samples.[10] The structural modifications which correspond to this nonlinear dependence are not clear. More studies are required to understand the nature of the superhard fullerite phases. Most of the previous studies have been concentrated on construction of a *P-T* diagram of C_{60} polymeric phases and included synthesis of many samples

with relatively poor characterization. Since this *P-T* diagram is now known in general, we concentrated instead on a detailed study of the most interesting part, wherein superhard phases (suggestively 3D polymerized fullerite) have been reported.

In this study, we present a detailed analysis of the samples obtained at 13 GPa and 830 K using XRD, Raman spectroscopy, and high-resolution transmission electron microscopy (HRTEM).

II. EXPERIMENT

A powder sample of C_{60} (99.9% purchased from MER Corporation) was pressurized to 13 GPa and heated at 830 K using a 5000 ton multianvil press. The samples were contained in a Pt capsule to avoid undesirable reactions with carbon. The sample assembly consisted of a MgO (+5 wt. % Cr_2O_3) octahedron (10 or 18 mm edge length) containing a $LaCrO_3$ heater. The octahedron was compressed using 54- or 32 mm tungsten carbide anvils with a truncation edge length of 11 or 4 mm, correspondingly, and pyrophyllite gaskets. The temperature was monitored with a $W_3Re/W_{25}Re$ thermocouple located axially with respect to the heater and with a junction close to the Pt capsule. The *P-T* uncertainties are estimated to be ±1 GPa and ±50 K, respectively. In each experiment, the sample was first compressed to the desired pressure; the temperature was then raised at ~100 K/min to the desired run temperature. Heating time for the first sample was 20 min and for the second sample 60 min. The samples were quenched by switching off the power to the furnace and then slowly decompressed. Upon completion of each experiment, the capsule was carefully removed and the treated material was mechanically cleaned of platinum. After quenching and pressure release, cylindrical samples with an approximate volume of 6 mm^3 were obtained. Sample 1 looked shiny and had very smooth surface on fresh cut. The second sample was less smooth and had some visible granular structure. Both samples appeared to be relatively hard and scratched the polished surface of cubic BN—the first sample especially easily.

The samples were characterized by XRD, Raman spectroscopy, and HRTEM. Hardness of the sample was measured using microindentor "Micro hardness tester" M-400-G2, Leco Corporation. A small piece was cut from the central part of sample 2 and loaded into a TAU-type DAC with 250-μm flat culets at nonhydrostatic conditions. NaCl powder was used as pressure-transmitting medium. This sample was pressurized up to 26 GPa. Two-dimensional XRD patterns of the sample were recorded *in situ* during the pressurizing and *ex situ* after quenching. The patterns were obtained with transmission geometry on the ID30 and BM01A beamlines at the European Synchrotron Radiation Facility (ESRF, Grenoble, France) with the MAR345 detector. The wavelengths of the x-ray beam were 0.3738 Å) and the beam size was 20×10 μm. The detector-to-sample distance was 350 mm. XRD images were taken with an incident x-ray beam parallel to the direction of compression ($\varphi=0°$). At some important points during heating and on quenched samples, XRD images were also taken with $\varphi=30°$ to determine presence of strong internal stress. This is necessary since previous studies showed that quenched samples prepared at similar conditions exhibited normal XRD rings with $\varphi=0°$ and strongly elliptical patterns due to the internal stress with $\varphi=90°$.[22] Recording XRD with $\varphi=90°$ (which should exhibit patterns with maximal ellipticity) is not possible inside a DAC; instead $\varphi=30°$ had to be used. This orientation could show smaller ellipticity of Debye-Scherrer rings compared to 90° geometry, but allows one to make a qualitative assessment as to whether patterns are elliptical or not. The collected images were integrated using the FIT2D program in order to obtain a conventional diffraction pattern. The XRD images were taken during pressurizing approximately at every 2–3 GPa, typically in several points close to the center of the hole. A Renishaw Raman 2000 spectrometer with a 785 nm laser was used to collect *ex situ* spectra of the studied sample. A low power was used to avoid laser-induced effects.

For TEM, the samples were crushed and then loaded in a suspension with ethanol onto a holey carbon grid. The sample was then inspected with a 200 kV Philips CM20 FEG-TEM, using HRTEM and selected-area electron diffraction (SAED) techniques. Additionally, we acquired electron energy loss spectra (EECS) of the C *K* edge, using the attached GATAN PEELS 666 spectrometer.

Sharp indentation experiments were performed using a Nano Indenter II™ (MTS Systems Inc., Oak Ridge, TN) nanohardness tester. A diamond Berkovich indenter with a tip radius of about 220 nm was used in experiments conducted with a maximum load of 5 mN. The loading and unloading phases of indentation were carried out under load control (nominal rate of 0.2 mN/s). At maximum load, a dwell period of 20 s was imposed before unloading, and another dwell period of 30 s at 80% of unloading to correct for thermal drift in the system. The adjacent indents were separated by at least 50 μm. The hardness and elastic modulus values are averaged over five measurements. Hardness and elastic modulus were calculated according to the Oliver and Pharr technique.[31]

III. RESULTS

A. XRD and HRTEM characterization of the sample

Structural characterization of sample 1 (heated for 20 min) by XRD and HRTEM appeared to be impossible due to the amorphous state of the material. The amorphous nature of this sample was also confirmed by Raman spectra, which will be discussed in more detail below.

Sample 2, obtained using a 1 h heating time, appeared to be crystalline and exhibited some interesting features in its Raman spectra. Therefore, an analysis of this sample is given below in more detail.

Analysis of XRD images taken *ex situ* on sample 2 showed normal circular Debye-Scherrer rings. No elliptic XRD patterns have been observed, unlike earlier studies by Marques *et al.*[22] The absence of ellipticity makes it easier to analyze conventional XRD patterns obtained by integration of 2D images (see Fig. 1). The measurements performed in different points of the sample showed, in general, very simi-

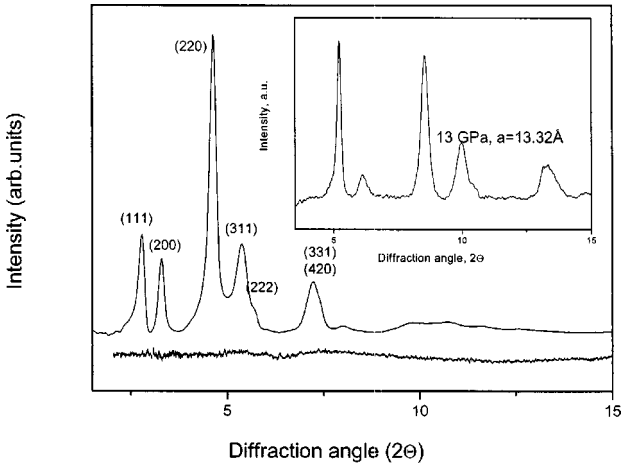

FIG. 1. XRD pattern recorded from the samples obtained by heat treatment of C_{60} at 13 GPa and 830 K for 1 h (top, sample 2) and for 20 min (bottom, sample 1, ×500). Inset shows XRD pattern recorded previously from the sample of C_{60} at 13 GPa and room temperature in diamond anvil cells (Ref. 12). The pattern given in the inset gives good approximation to the state of sample 2 prior heating. The wavelengths of the x-ray beam were 0.3738 Å for the samples 1 and 2, and 0.7 Å for the pattern shown in the inset.

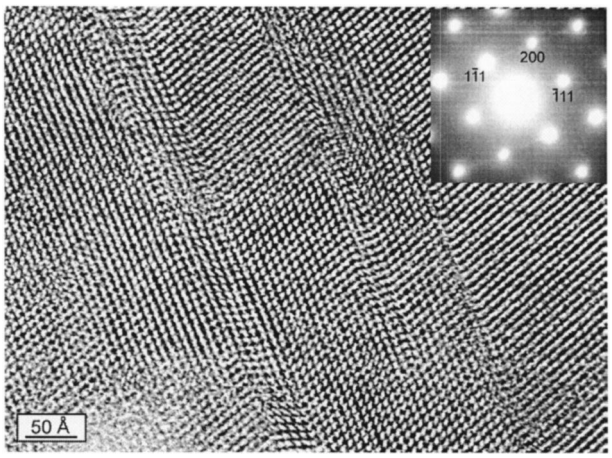

FIG. 2. HRTEM image of fcc structured C_{60} with microtwins and stacking faults parallel to (111). The inset shows a SAED pattern with streaks along the $[111]^*$ direction.

lar patterns that can be indexed as fcc, but the cell parameter was found to be slightly different in different points: $a = 13.07-13.39$ Å. It shall be emphasized that this cell parameter was measured after a decrease of temperature and release of pressure. The value of this cell parameter is unknown at HPHT conditions, or whether it has changed significantly after return back to ambient conditions. Other studies suggest that this change is usually not very strong.[13]

The value of smallest observed cell parameter ($a = 13.07$ Å) corresponds to a cell volume per C_{60} molecule of 558 Å^3. This is in good agreement with our previous *in situ* study conducted in a DAC.[12,13] It shall be noted that the quality of fit is not very high, with a cell volume standard deviation of about 19.6 Å^3. This means that the cubic cell is slightly distorted, most probably due to the stress influence, and allows in principle a rhombohedral interpretation. A rhombohedral fit gives a somewhat better cell volume deviation but XRD does not exhibit any additional peaks from this rhombohedral structure. Therefore, in this study the cubic structure will be used in the following, although it is certainly slightly distorted. The cubic structure was also found using HRTEM experiments, which are described below. In our previous study it was suggested that the decrease of the cell volume per molecule can be used to assess the approximate number of intercage connections in C_{60} polymeric phases.[13] Following the trend of volume per molecule decrease of about 20 Å^3 for each new square ring connecting neighboring molecules, the volume of 558 Å^3 will corresponds to a polymer with eight square rings per C_{60} molecule. Such a polymer must have a 3D structure. The value of highest observed cell parameter $a = 13.39$ Å corresponds to cell volume per molecule of 600 Å^3. This volume is similar to the value known for the 2D rhombohedral polymeric phase produced at pressures below 9 GPa. The structure of our sample is clearly different from 2D polymers. Similar volumes allow us to suggest that the sample in this region could have six square-ring connections per molecule. In principle, it is possible to imagine different kinds of 3D geometry for six square connections as well. Summarizing this part, analysis of XRD data allows us to suggest that sample 2 could be interpreted as a polymer with 6–8 square connections per C_{60} molecule.

For comparison, Fig. 1 (see inset) also shows the XRD pattern of C_{60} at 13 GPa from our previous study recorded prior to the heating *in situ* in the DAC. Although stress conditions are slightly different in the DAC compared to the multianvil cell, this XRD pattern must describe with good approximation the state of our sample prior to heating. As can be seen in this figure, the heated sample shows different relative intensities for XRD peaks and a smaller cell parameter. According to *in situ* data, the cell parameter of a sample treated at 13 GPa and 830 K is only slightly changed after quenching and pressure release.[13] Therefore, most probably the cell parameter of our sample prior to cooling must have been only slightly smaller than the final value of $a = 13.07-13.39$ Å obtained after quenching and pressure release.

Additional structural information was also obtained using HRTEM. The TEM observations reveal that sample 2 is fcc structured with $a = 13.36$ Å, which is in good agreement with XRD data. HRTEM images show that the C_{60} polymorph contains numerous microtwins and stacking faults on (111) (Fig. 2). These planar defects cause the streaking visible along the $[111]^*$ direction in the SAED pattern. Such defects are typical of fcc- or diamond-structured materials. In general, the packing of the C_{60} molecules is rather good according to Fig. 2. Surprisingly, this figure does not reveal any proof for 2+2 cycloaddition polymerization in the C_{60} material. Previous experiments with C_{60} performed at 12–14 GPa also showed that the fcc phase persists at least up to 800 K.[10,13,32] The significant decrease of the cell parameter of the fcc structure was typically explained by the formation of chain polymers chaotically arranged in all directions, which, on average, gives a "pseudocubic" structure. This explanation fits well to our XRD data, but is in dis-

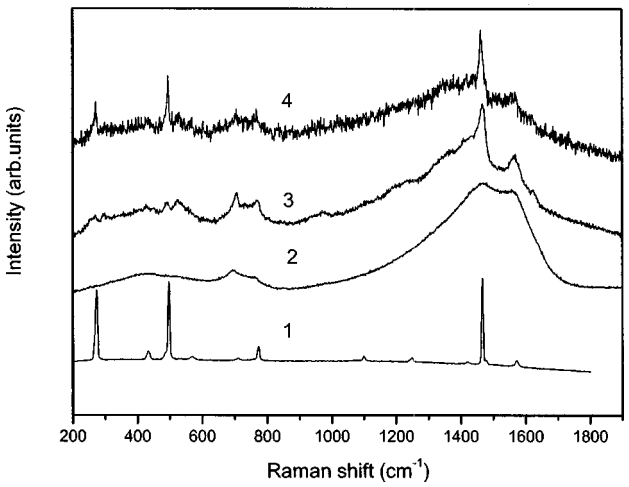

FIG. 3. Raman spectra recorded from the pristine C_{60} (curve 1), sample 1 (curve 2), sample 2 at low laser power (3), and Sample 2 at higher laser power, which resulted in appearance of peaks from pristine C_{60}.

agreement with HRTEM. Random chain polymerization could produce fcc structure on the macro level, but on the micro level, the structure must be of smaller symmetry due to a lower intermolecular distance between molecules connected by polymeric square rings.

In order to check the nature of the material and kind of bonding in the sample 2, EELS experiments were also performed. This method allows to determine directly the degree of sp^2/sp^3 hybridization in carbon materials. It is known that the degree of sp^3 hybridization is increased due to 2+2 cycloaddition. Therefore, C *K* EELS taken from sample 2, original C_{60} and rhombohedral polymer of C_{60} were compared.

Measurements showed a very complex electron energy loss near-edge structure (ELNES), reflecting differences in the local environment of carbon atoms. However, the ELNES spectra of starting and synthesized materials look identical, suggesting that the local environment of carbon atoms is unaffected by the high pressure experiment and that the carbon buckyballs remain intact. Unfortunately, no conclusions about change of degree for sp_2/sp_3 hybridization could be drawn from the ELNES spectra. The spectra taken from the rhombohedral C_{60} polymer appeared to be identical to the spectra of pristine C_{60} and sample 2. The expected increase in sp_3 hybridization due to formation of polymeric bonds is possibly too small to be detected by EELS.

B. Raman characterization of the samples

The Raman spectra of the studied samples are shown in Fig. 3. Since the samples were relatively large, Raman spectra were recorded in many points, including the cylindrical outer surface and the core part on a fresh cut. The quality of the spectra recorded in the different points was not the same. Some points exhibited spectra with stronger peaks, some points with weaker, but in general both samples seem to be rather homogeneous; there is no difference, for example, between core region of the sample and its surface.

Sample 1 exhibited only several broad features in the Raman spectra, but analysis of these peaks seems to present interesting results (see Fig. 3). This spectrum shows some strong differences compared to the typical Raman spectra of superhard phases published in the literature. Typically, reported superhard phases exhibited only two broad peaks: the main one centered approximately at 1563 cm^{-1} and the second low-intensity feature at 500–800 cm^{-1} (see, for example, Refs. 13, 14, and 28). In the spectrum recorded from Sample 1 the picture is more complex: the broad peak centered at 1563 cm^{-1} is also observed, but is weaker compared to the main peak centered approximately at 1467 cm^{-1}. There are also broad peaks at 696 and 763 cm^{-1} and some broad features at around 430 cm^{-1}. Peaks at 696 and 763 cm^{-1} are certain proof that at least part of the fullerene molecules is still intact in the studied sample. Usually these peaks are attributed to vibrations derived from the $H_g(3)$ and $H_g(4)$ modes of pristine C_{60}. The peak at 1467 cm^{-1} shall be interpreted as an extremely broad $A_g(2)$ mode, which possibly includes also the $H_g(7)$ mode (which can be recognized from the asymmetric shape of the feature). It shall be emphasized that if this interpretation is true, the $A_g(2)$ mode in Sample 1 shows no downshift compared to pristine C_{60} (found usually at 1467–1469 cm^{-1} depending on the used laser). The absence of a strong downshift in position of the $A_g(2)$ mode would be rather unexpected for 3D C_{60} polymer. This observation is in contradiction with the known trend in the $A_g(2)$ mode position for 1D and 2D polymers, which suggests stronger downshift for more strongly polymerized materials. Typically, peaks found at 900–1000 cm^{-1} spectral region are considered as a sign for the 2+2 mechanism of polymerization[4–6] but the spectrum of sample 1 shown in Fig. 3 does not show any clear features here. In general, it can be speculated that the observed spectrum shows no clear proofs for the 2+2 cycloaddition mechanism of polymerization and could represent only very strongly stressed molecules of C_{60}. Unfortunately, the amorphous state of the sample does not allow us to compare Raman and XRD data in order to explain the nature of the sample, which will be discussed again below.

Comparison of the results obtained from Raman data and structural information from XRD and HRTEM is possible for sample 2, which is discussed in more detail below. Raman peaks from the fullerite phase are much sharper in the spectra recorded from sample 2 compared to those observed in sample 1. This result is in good agreement with the better crystal packing revealed by XRD of sample 2.

The spectrum recorded from sample 2 with low laser power exhibits several peaks from the fullerite phase that are significantly broader compared to the reference C_{60} spectrum (see Fig. 3). The position of the $A_g(2)$ mode is found at 1468 cm^{-1} similar to the untreated C_{60}, but at the same time a number of new peaks is observed which suggest that the sample has a polymeric structure. In fact, the $A_g(2)$ peak is not only much broader compared to pure C_{60}, but is also asymmetric, with some shoulders about 1435 and 1441 cm^{-1}. Judging only from Raman spectra, it would be possible to suggest that this sample consists of a mixture of monomeric C_{60} with the addition of chain and 2D polymers.

This suggestion, though, is not compatible with all the other data. The relatively high hardness and density of the sample provide evidence for stronger polymerization of the sample with a higher number of intercage bonds compared to 1D and 2D polymers. Typically, polymeric phases of C_{60} show downshifts of the $A_g(2)$ mode proportionally to the number of square rings connecting neighboring molecules. The strongest downshift is observed for the rhombohedral polymer with six square rings per molecule (about 60–63 cm^{-1}). Following trivial logic, addition of more polymeric bonds could be expected to result in an even stronger downshift of the $A_g(2)$ mode. The studied sample shows all signs of the increased degree of polymerization, such as higher density and hardness, but the $A_g(2)$ mode is not downshifted compared to untreated C_{60}. Therefore, it is possible to suggest that the $A_g(2)$ mode downshift trend observed for 1D and 2D C_{60} polymers does not expand to 3D structures. The reasons for such a phenomenon are not clear at the moment. One possibility is that downshift of the $A_g(2)$ mode is connected only to planar distortion of the C_{60} molecule and disappears if intermolecular connections are distributed randomly over all the molecule in three dimensions.

Additional proof that the studied sample has polymeric structure was obtained by recording spectra with increased laser power. The heating produced by the laser results in decomposition of polymeric phase into pristine C_{60}, which can be detected by appearance of sharp peaks of $H_g(1)$, $A_g(1)$, and $A_g(2)$ modes in their normal positions (see Fig. 3, curve 4). A stronger increase of laser power resulted in burning of the sample with formation of two broad features typical for Raman spectra of amorphous graphite-like carbon.

Concluding this discussion, the Raman spectra of sample 2 showed a rather complex picture: the clearly present evidence for the presence of unbroken C_{60}, but shows no proof for the formation of a 3D polymer by 2+2 cycloaddition mechanism, which is suggested from the relatively small cell parameter obtained from XRD. Looking only into the Raman data, one could draw the conclusion that the sample consists of a mixture of monomeric, dimeric, and a relatively small fraction of 2D polymers. Such a conclusion would be in contradiction with XRD and TEM data, which show only a fcc cubic phase and no other lower symmetry structures typical for known C_{60} 1D and 2D polymers. The strong but broad peak at 1468 cm^{-1} suggests again the possible presence of strongly stressed but nonpolymeric C_{60} as a major component of the sample, similar to sample 1.

C. Hardness measurements

Hardness studies of the samples must provide some crucial information to explain the mechanism of phase transformations in samples 1 and 2. If the hardness of a sample is high, this shall be considered as evidence for formation of rigid covalent bonds connecting neighboring molecules in a 3D network, while 1D and 2D polymers of C_{60} are known to be soft.

Hardness measurements were first attempted using the microindentation method. Sample 1 appeared to be too hard for measurement: no visible indentation was observed with a small load, and with a higher load the sample cracked. This is in good agreement with the high hardness of the sample which was obvious from easy scratching of cubic BN.

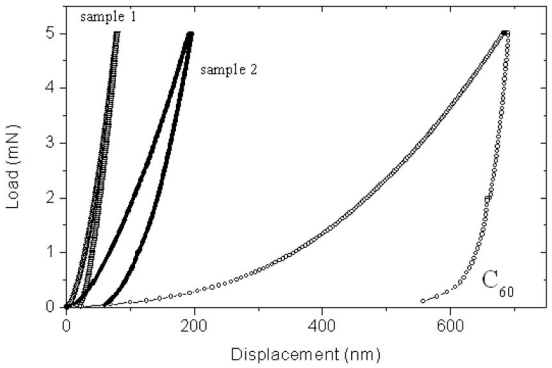

FIG. 4. Typical load-displacement curves for samples 1 and 2 (heated at 13 GPa and 830 K for 20 and 60 min, respectively) compared to pristine C_{60}.

Sample 2 exhibited much more complex behavior. The sample also scratched cubic BN, but with some difficulty. According to measurements performed using the microindentor, the hardness of this sample is about 37 GPa. It shall be noted that this value was obtained only when a relatively small load below 1.3 g was used for indentation. At a higher load (>10 g), the fullerite phase obviously collapsed during indentation, which resulted in a low hardness of 1–2 GPa. Collapse of the fullerite phase was also detected by Raman spectroscopy. The Raman spectrum typical for the studied sample (see Fig. 2) and discussed below was replaced after indentation by the spectrum of pristine C_{60}. Obviously, the material in sample 2 is at metastable conditions that can be spontaneously released either by heating with the Raman laser (see above) or by stress from the microindentor tip. One possible explanation for this transformation suggests breaking of polymeric bonds (3D polymer unstable at ambient conditions). More precise hardness measurements were performed using the nanoindentation method (see Fig. 4). The Young modulus and hardness of Sample 1 calculated from Fig. 4 are 436 GPa and ~45 GPa, respectively. For the Sample 2 these values are 69 GPa for Young's modulus and 6.8 GPa for the hardness. The hardness value measured by the nanoindentor for sample 1 is in the good agreement with the previously discussed microindentor test, but for sample 2 the difference between the two measurements is too high. One possibility to explain the difference is that hardness measurements using the microindentor with small load (<1.3 g) could result in overestimation of hardness:[32] On the other hand, the effect of a transformation into pristine C_{60} (observed using the microindentor at higher load) could be responsible for the underestimated hardness when nanoindentation was used. The load force in the nanoindentor tests was not much higher compared to microindentation method, but possibly the transformation is caused mostly by stress created locally in the sample. This stress is possibly higher when nanoindentation is used, which could explain the ob-

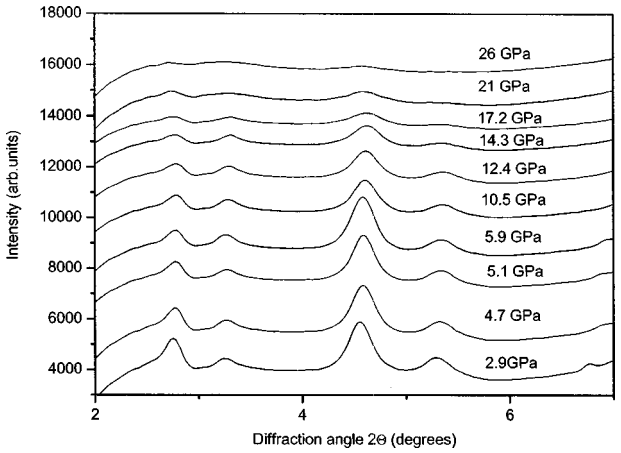

FIG. 5. *In situ* XRD patterns recorded for sample 2 during pressurizing up to 26 GPa using synchrotron radiation.

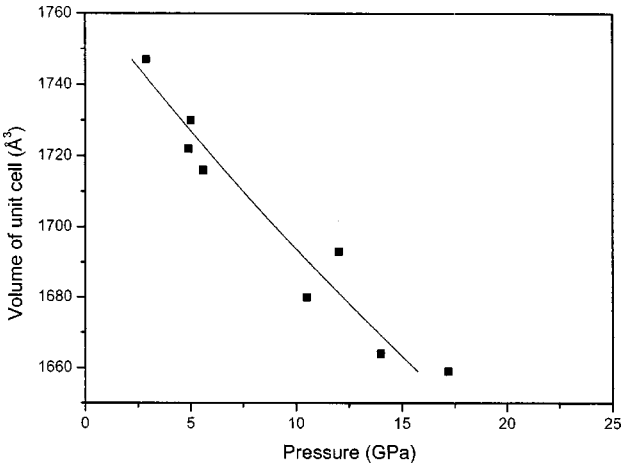

FIG. 6. Experimental points from *in situ* compression experiments (unit cell volume vs pressure) fitted with Birch-Murnaghan equation ($K=217$, $V_0=2371$).

served difference. Possible reasons for such behavior will be discussed below in Sec. IV. In order to check the stiffness of the sample by an independent method, compression experiments using synchrotron radiation were performed. Results of these experiments are presented below.

One of the main differences of our sample compared to previous studies in the same *P-T* region (800 K and 13 GPa) is the relatively large cell parameter and the relatively low density of the sample. The density calculated from the XRD data is 2.15 g/cm^3. This density and the cell parameter values are in good agreement with the moderately high hardness of the sample.

D. *In situ* XRD synchrotron compression study up to 26 GPa

The compression study of sample 2 synthesized by heat treatment at 13 GPa and 830 K for 1 h was performed in a DAC. The characterization of the sample prior to compression is described above. According to the data obtained by HRTEM and XRD the sample at ambient conditions is cubic, with cell parameter of 13.07–13.36 Å depending on the point of measurement. The XRD patterns obtained during pressurizing up to 26 GPa are shown in Fig. 5. In the particular point of the sample where this measurement was performed, the starting cell parameter was $a=13.25$ Å. As can be seen in this figure the XRD patterns show very small changes up to 17 GPa and quick amorphisation above 20 GPa. Some trace amounts of crystalline phase still can be detected up to 26 GPa, but only very few peaks are available for analysis. The interpretation of these patterns shows that the sample remains cubic during compression, since no new peaks appear at higher pressures. It shall be noted that the quality of fit became less and less good during compression, which is evidence for distortion of cubic cell. As it was noted above, rhombohedral indexing gives a slightly better cell volume standard deviation σ compared to a cubic fit, but the difference between cubic and rhombohedral fits remains almost the same during compression and no new peaks appeared. Therefore, it is easier to describe the sample as distorted cubic rather than rhombohedral. The minimal cell parameter was observed at 17 GPa ($a=13.02$ Å). Some traces of XRD peaks can still be detected at patterns recorded at 21 and 26 GPa, but they become very broad and weak. Interpretation of so poor patterns is rather ambiguous and they were not used for cell parameter evaluation. The evolution of the relative cell volume during pressurizing was extracted from the data shown in Fig. 5. Fitting the curve up to 17 GPa was performed using the Birch-Murnaghan equation. The K' was constant and equal to 4. The errors are relatively high due to slightly inhomogeneous nature of sample. Fitting resulted in a bulk modulus value of 217(10) GPa and $V^0=1763.9(5)$ for the studied sample (see Fig. 6). This value of bulk modulus is smaller than the bulk modulus of diamond (441 GPa), but much higher compared to available data on 2D C_{60} polymers (34.8 GPa for the tetragonal phase). The bulk modulus obtained from our compression experiment is in good agreement with the moderately high hardness of 37 GPa measured using the microindentation method.

The two patterns recorded above 20 GPa (see Fig. 5) were not suitable for cell parameter determination. The fitting of these XRD patterns is rather poor due to the low intensity and number of peaks. Most probably this phenomenon can be explained by collapse of the fullerite phase with formation of very dense amorphous phase.

It shall be noted that similar experiments were performed very recently by Mezouar *et al.*,[33] but their sample of suggestively 3D C_{60} polymer had a higher density (2.7 g/cm^3), a higher bulk modulus of 288 GPa and a huge internal stress resulting in elliptical Debye-Scherrer XRD patterns. In the case of our studies, no elliptical XRD patterns were observed and analysis was more easy.

IV. DISCUSSION

The two studied samples were synthesized at 13 GPa and 830 K, but using different heating time: 20 and 60 min, respectively. Results presented above prove that C_{60} molecules are unbroken in both of the samples. In the case of sample 2, it is not only evident from XRD and Raman spectroscopy, but also directly proved by HRTEM imaging. Since the

Sample 1 was synthesized at the same *P-T* conditions, but with a shorter heating time, it can be considered as a preliminary step for synthesis of sample 2. Therefore, it also must consist of unbroken C_{60} molecules. The second important observation is that longer heating time resulted in crystallization of the material and a decrease of hardness. Sample 2 exhibited relatively good XRD patterns, while Sample 1 was amorphous and exhibited no diffraction peaks even when synchrotron radiation was attempted for recording patterns.

The most interesting question to be solved is the nature of the studied samples. The study of sample 1 has not provided much structural information, but the second sample allows us to discuss the phase transformations of C_{60} at 830 K and 13 GPa in more detail. The main trend in the phase transformation is similar to the literature data: during the heating at 13 GPa the structure remains fcc but the cell parameter is decreased.[9,10,13,34]

The cell parameter value of $a=13.07$ Å obtained for sample 2 corresponds to center-to-center distances between C_{60} molecules of 9.24 Å. This shall be compared to the nearest neighbor distance in polymers formed by 2+2 cyloaddition (9.09–9.14 Å) and of single-bonded Na_4C_{60} (reported to be 9.28 Å). Therefore, Sample 2 was compressed to the distance between C_{60} molecules where polymerization could occur in three dimensions by formation of single bonds. This kind of bonding has never been observed for undoped C_{60}, but cannot be ruled out as a possibility. On the other hand, experimental values of intermolecular distance are close enough to 2+2 cycloaddition to be reasonably explained by this mechanism if only part of material is polymerized in three dimensions, with remaining part consisting of randomly linked chains. Another possibility is that there is an unknown mechanism of bonding in sample 2, different from the 2+2 cycloaddition mechanism.

It is commonly believed that polymerization at 13 GPa during the heating starts as chain formation. Well ordered chain polymer is known to exhibit an orthorhombic structure, but if the chains are formed chaotically in all directions, it could result in an average pseudocubic structure with decreased cell parameter. Linking these chains to each other will result according to this mechanism in formation of 3D polymers. Such a pseudocubic structure could explain our XRD data, because XRD is a macro method which averages data over a significant volume of material. For the HRTEM, however, this is not the case. If chaotic chain formation occurs in the sample, it must be seen by HRTEM as local deviations from the cubic structure. Intermolecular covalent bonds results in a decrease of the distance between C_{60} molecules, which must be detected by HRTEM images.

In the second sample studied in the present work, the structure according to both XRD and HRTEM remains fcc cubic while the cell parameter is decreased to 13.07–13.36 Å compared to the original 14.17 Å for pristine C_{60}. A surprising result is that no evidence for polymerization can be found in this sample from HRTEM. The packing of C_{60} molecules is very clearly fcc without any specific changes that would have been seen if polymeric chains were present in this sample. Paradoxically, the structure of the sample looks as if it was original fcc C_{60} without covalent intermolecular bonds, but with a smaller cell parameter. The next question is why the C_{60} molecules keep closer to each other if there are no covalent intermolecular bonds. Some compression under pressure is reasonable for pristine C_{60} with van der Waals bonding between molecules. Since the molecules cannot rotate at 13 GPa, they could not find proper orientation, and therefore polymeric bonds could not form. There is nothing unusual until that point. The question is why the cell parameter has remained smaller after return from HPHT back to normal conditions. This can be explained only by the existence of rigid intermolecular bonds connecting neighboring molecules, which is also responsible for increased hardness of the sample.

Unfortunately, the presence of 2+2 cycloaddition mechanism could not be verified by EELS since the difference in degree of sp_2/sp_3 hybridization due to the formation of intermolecular bonds appeared to be too low for the sensitivity of this method. Raman spectroscopy also does not clearly confirm the presence of covalent intermolecular bonds: in both samples 1 and 2 the main peak from the $A_g(2)$ mode is not downshifted, but only significantly broadened. In principle, this can be interpreted as strongly stressed nonpolymeric C_{60}. Some traces of polymerization can be seen in the Raman spectra of sample 2, but certainly only as minor component. It is also clear that some second amorphous carbon phase is present in the samples: a broad peak at 1563 cm^{-1} for the sample 1 and some broad background in the spectra of sample 2 are evident from Fig. 3.

It is also rather interesting that the transformation back to normal C_{60} can be induced in sample 2 either by heating with laser light or by stress from the microindentor. This clearly proves that the C_{60} structure in sample 2 is metastable. It is interesting to note that a somewhat similar explosive transformation under laser light was reported by Meletov *et al.* for a probably 3D polymer of C_{60}.[35]

As was noticed above, strong compression of the C_{60} structure without formation of covalent bonds under high-pressure conditions is possible due to geometrical frustrations since molecules do not rotate at 13 GPa. This was proved in one of the earliest studies of C_{60} under high-pressure conditions. As was shown by Duclos *et al.*,[25] compression using pseudohydrostatic conditions (using DAC) was remarkably higher compared to the experiment performed without a pressure-transmitting medium. In our experiment, conditions were close to hydrostatic. The multianvil press most likely provides the best approximation to hydrostatic conditions compared to all other high-pressure methods. Therefore, at 13 GPa and prior to heating, the C_{60} sample was compressed for $V/V_o \sim 0.74$ without formation of polymeric bonds. Although the distance between C_{60} molecules at this point is small enough for formation of polymeric bonds, the orientation of molecules is random and proper orientation cannot be achieved due to the absence of molecular rotation in the compressed state. During the heating some additional linking must occur in the sample, which is evident from the irreversible character of the transformation. The cell parameter of the C_{60} material remains smaller even when quenched and after the pressure release. The nature of the linking mechanism between C_{60} molecules in such material is not quite clear. Results obtained in this study show some problems in application of the 2+2 cycloaddition

polymerization mechanism for C_{60} compressed to 13 GPa and heated at 830 K.

The cell parameter of our sample is significantly larger compared to the data reported by other research groups at the same *P-T* conditions: 13.07 Å compared to 12–12.5 Å in some other studies.[9,10,22] We believe that this difference is mostly not due to experimental errors but is rather due to some features typical for each experimental method. Until now, the following methods were used for HPHT region around 13 GPa and 830 K: "toroid"-type chamber, DAC, and multianvil presses. Below, some important parameters of HPHT treatment and some particularities typical for each experimental method in connection with these parameters are discussed in more detail.

As was shown in some previous studies, the results of HPHT experiments depend not only on the particular *P-T* point where the synthesis was performed, but also on other factors, most importantly stress conditions, heating time, and the *P-T* history of treatment.[10,13,34,35] All these factors should be taken into account when experimental data obtained by different groups are compared.

The time of heat treatment studied in the recent work by Horikawa *et al.*[10] seems to be especially important for interpretation of HPHT results. It was found that longer heating is not necessary to produce harder samples. Indeed, there is a time limit of 60 min, after which the samples become softer. The study of Horikawa performed at 12 GPa and 650 K shows a maximum hardness at about 20 min. This maximum of hardness is shifted towards longer heating time at lower temperature. It seems that, for every set of specific *P-T* conditions, the maximum hardness is achieved with a different heating time.

This can explain some drastic hardness differences reported in literature. The samples with hardness comparable to or higher than diamond (100 GPa) have been obtained by Blank *et al.* at 13 GPa and 830 K with a heating time of 1 min.[14] The same heating time was used in experiments by Brazkin *et al.* at 12.5 GPa and different temperatures, and their sample exhibited very high hardness up to 87 GPa.[21] It should be noted that the short time of heating (1 min) in the above studies resulted in strongly inhomogeneous samples. In the experiments presented in this study, the heating time was increased to 1 h and the hardness appeared to be much lower (37 GPa). The same is true for our previous experiments in DACs, where heating was performed over a long period of time (8–9 h), and resulted in samples with hardness below 40 GPa.[11,13] Therefore, difference between our data and the data obtained by Blank *et al.* and Brazkin *et al.* can be explained mostly by the difference in heating time, taking into account results by Horikawa *et al.*[10]

The difference in heating time cannot by itself explain all observed divergence of published experimental results. Another important parameter is stress. It is more difficult to compare stress conditions used in different experiments. For example, the toroid chamber apparatus used in studies by Blank *et al.* must have very strong stress conditions during the synthesis. Precise pressure and temperature control was hardly possible in these pioneering studies, which resulted in highly inhomogeneous samples (density variations within 2.2–3.4 within the same sample[23]). The multianvil press most likely provides the best approximation to hydrostatic conditions compared to other high-pressure experiments—in the DAC (without hydrostatic or with solid pressure medium) and in toroidal press, where the chamber may provide strong stress conditions.[10,34,36]

In general, the increased stress favors C_{60} polymerization. Experiments with rotation anvils revealed that under strong shear stress, the superhard fullerite phase can be produced even at room temperature.[37] Strong stress could explain why Blank *et al.*[14] could obtain superhard material using a very short heating time, while Horikawa *et al.* observed maximum hardness with a longer heating time.[10] Intermediate stress conditions are probably typical for experiments with DACs (when no rotation of anvils is used). Even when some pressure medium is used in DAC experiments, the conditions shall be described as quasihydrostatic, since only solid materials such as NaCl can be used at 13 GPa [all liquid media such as a methanol-ethanol mixture solidify at lower pressure (and ambient temperature)]. Using a pressure medium at high temperature could also be risky due to the possibility of chemical reaction with C_{60} (as in a case of ethanol-methanol, for example). Of course, using no pressure transmitting media shall increase stress. This can explain why in our previous experiments we observed a clear distortion of cubic structure to rhombohedral during HPHT treatment around 13 GPa and 830 K.[13] The stress and therefore distortion was even stronger in experiments performed by Blank *et al.* using the toroid method, which probably could explain why in some studies their samples were interpreted using low-symmetry structures (orthorhombic or monoclinic; see, for example, Ref. 23). The stress typical for this method was so strong that residual shear deformation resulted in elliptical Debye-Scherrer XRD patterns recorded from such samples.[22] These ellipses were not observed in other samples obtained by different methods even when the same *P-T* conditions were used for synthesis. It was clearly shown that elliptical XRD patterns are not a signature of superhard fullerite and can be observed even for 2D polymeric phases if stress was high.[38] Of course, the experiments performed using shear diamond anvil cells (SDACs)[16–18] shall be considered as a very special case due to very strong stress intentionally created in this method. Most probably, *P-T* diagrams constructed using SDACs cannot be directly compared to other *P-T* diagrams constructed from the data obtained at low-stress conditions.

Finally, the heating and pressurizing pathway (treatment history) influences the outcome of experiments. It was shown in many studies at pressures below 10 GPa that an increase of pressure followed by heat treatment produces samples with different phase compositions compared to the case when the temperature was increased first, followed by pressurizing. The same is true for the high-pressure region above 12 GPa as well, as was recently discovered.[33,39]

The above discussion leads to conclusion that the seemingly contradictory data presented by different groups for the pressure region above 13 GPa can be explained when differences in heating time, stress conditions, and history of treatment are taken into account.

In conclusion, both studied samples (heated at 13 GPa and 830 K for 20 min and for 1 h) consist of unbroken C_{60}

molecules. Longer heating results in crystallization of amorphous material. The data obtained by XRD, Raman, and HR-TEM cannot be explained by the previously suggested model of random chain polymerization. Decreased cell parameter and high hardness of the high-pressure phase (sample 2) provide evidence for strong intermolecular bonding in the structure. On the other hand, no clear evidence for a 2+2 polymerization mechanism can be found in results obtained by characterization methods used.

ACKNOWLEDGMENTS

The authors gratefully acknowledge useful discussion and proofreading of the paper by Prof. Bertil Sundqvist.

*On leave from Uppsala University, Department of Materials Chemistry, Angström Laboratory, Box 538, SE-751 21, Uppsala, Sweden.

[1] M. Núñez-Regueiro, L. Marques, J.-L. Hodeau, O. Bethoux, and M. Perroux, Phys. Rev. Lett. **74**, 278 (1995).
[2] A. M. Rao, P. C. Eklund, J.-L. Hodeau, L. Marques, and M. Nunez-Regueiro, Phys. Rev. B **55**, 4766 (1997).
[3] V. A. Davydov, V. Agafonov, H. Allouchi, R. Céolin, A. V. Dzyabchenko, and H. Szwarc, Synth. Met. **103**, 2415 (1999).
[4] V. A. Davydov, L. S. Kashevarova, A. V. Rakhmanina, V. M. Senyavin, R. Céolin, H. Szwarc, H. Allouchi, and V. Agafonov, Phys. Rev. B **61**, 11 936 (2000).
[5] B. Sundqvist, Adv. Phys. **48**, 1 (1999).
[6] T. Wågberg, P.-A. Persson, and B. Sundqvist, J. Phys. Chem. Solids **60**, 1989 (1999).
[7] R. A. Wood, M. H. Lewis, G. West, S. M. Bennington, M. G. Cain, and N. Kitamura, J. Phys.: Condens. Matter **12**, 10411 (2000).
[8] L. Marques, M. Mezouar, J.-L. Hodeau, and M. Nunez-Regueiro, Phys. Rev. B **68**, 193408 (2003).
[9] S. M. Bennington, N. Kitamura, M. G. Cain, M. H. Lewis, R. A. Wood, A. K. Fukumi, and K. Funakoshi, J. Phys.: Condens. Matter **12**, 451 (2000).
[10] T. Horikawa, K. Suito, M. Kobayashi, and A. Onodera, Phys. Lett. A **287**, 143 (2001).
[11] A. V. Talyzin, L. S. Dubrovinsky, and T. Le Bihan, U. Jansson, J. Chem. Phys. **116**, 2166 (2002).
[12] A. V. Talyzin, L. S. Dubrovinsky, T. Le Bihan, and U. Jansson, Phys. Rev. B **65**, 245413 (2002).
[13] A. V. Talyzin, L. S. Dubrovinsky, M. Oden, T. Le Bihan, and U. Jansson, Phys. Rev. B **66**, 165409 (2002).
[14] V. D. Blank, S. G. Buga, N. R. Serebryanaya, V. N. Denisov, G. A. Dubitsky, A. N. Ivlev, B. N. Martin, and M. Yu. Popov, Phys. Lett. A **205**, 208 (1995).
[15] V. Blank, M. Popov, S. Buga, V. Davydov, V. N. Denisov, A. N. Iblev, B. N. Mavrin, V. Agafonov, R. Ceolin, H. Szwarc, and A. Rasat, Phys. Lett. A **188**, 281 (1994).
[16] V. D. Blank, S. G. Buga, N. R. Serebryanaya, G. A. Dubitsky, S. N. Sulyanov, M. Yu. Popov, V. N. Denisov, A. N. Ivlev, and B. N. Martin, Phys. Lett. A **220**, 149 (1996).
[17] V. D. Blank, S. G. Buga, N. R. Serebryanaya, G. A. Dubitsky, R. H. Bagramov, M. Yu. Popov, V. M. Prokhorov, and S. A. Sulyanov, Appl. Phys. A: Mater. Sci. Process. **64**, 247 (1997).
[18] V. D. Blank, S. G. Buga, N. R. Serebryannaya, G. A. Dubitsky, B. N. Mavrin, M. Yu. Popov, R. H. Bagramov, V. M. Prokhorov, S. N. Sulyanov, B. A. Kulnitsky, and Ye. V. Tatyanin, Carbon **36**, 665 (1998).
[19] V. D. Blank, S. G. Buga, G. A. Dubitsky, N. R. Serebryanaya, M. Yu. Popov, and B. Sundqvist, Carbon **36**, 319 (1998).
[20] V. V. Brazkin, A. G. Lyapin, S. V. Popova, Yu. A. Klyuev, and A. M. Naletov, J. Appl. Phys. **84**, 219 (1998).
[21] V. V. Brazkin, A. G. Lyapin, S. V. Popova, R. N. Voloshin, Yu. V. Antonov, S. G. Lyapin, Yu. A. Kluev, A. M. Naletov, and N. N. Melnik, Phys. Rev. B **56**, 11 465 (1997).
[22] L. Marques, M. Mezouar, J.-L. Hodeau, M. Nunez-Regueiro, N. R. Serebriannaya, V. A. Ivdenko, V. D. Blank, and G. A. Dubitsky, Science **283**, 1720 (1999).
[23] L. A. Chernozatonskii, N. R. Serebryanaya, and B. N. Mavrin, Chem. Phys. Lett. **316**, 199 (2000).
[24] N. R. Serebryanaya and L. A. Chernozatonskii, Solid State Commun. **114**, 537 (2000).
[25] S. J. Duclos, K. Brister, R. C. Haddon, A. R. Kortan, and F. A. Thiel, Nature (London) **351**, 380 (1991).
[26] E. Burgos, E. Halac, R. Weht, H. Bonadeo, E. Artacho, and P. Ordejon, Phys. Rev. Lett. **85**, 2328 (2000).
[27] F. Moshary, N. Chen, I. F. Silvera, C. A. Brown, H. Dorn, S. De Vries, and D. S. Bethune, Phys. Rev. Lett. **69**, 466 (1992).
[28] C. S. Yoo and W. J. Nellis, Chem. Phys. Lett. **198**, 379 (1992).
[29] A. V. Talyzin, L. S. Dubrovinsky, M. Oden, and U. Jansson, Diamond Relat. Mater. **10**, 2044 (2001).
[30] A. V. Talyzin, L. S. Dubrovinsky, and U. Jansson, Phys. Rev. B **64**, 113408 (2001).
[31] W. C. Oliver and G. M. Pharr, J. Mater. Res. **7**, 1564 (1992).
[32] V. Brazhkin, N. Dubrovinskaia, M. Nico, N. Novikov, R. Riede, V. Solozhenko, and Y. Zhao, Nat. Mater. **3**, 576 (2004).
[33] M. Mezouar, L. Marques, J.-L. Hodeau, V. Piscedda, and M. Nunez-Regueiro, Phys. Rev. B **68**, 193414 (2003).
[34] R. A. Wood, M. H. Lewis, S. M. Bennington, M. G. Cain, N. Kitamura, and A. K. Fukumi, J. Phys.: Condens. Matter **14**, 11615 (2002).
[35] K. P. Meletov, S. Assimopoulos, I. Tsilika, G. A. Kourouklis, J. Arvanitidis, S. Ves, B. Sundqvist, and T. Wågberg, Chem. Phys. Lett. **341**, 435 (2001).
[36] M. Eremets, *High Pressure Experimental Methods* (Oxford University Press, New York, 1996).
[37] N. R. Serebryanaya, V. D. Blank, V. A. Ivdenko, and L. A. Chernozatonskii, Solid State Commun. **118**, 183 (2001).
[38] L. Marques, M. Mezouar, J.-L. Hodeau, and M. Núñez-Regueiro, Phys. Rev. B **65**, 100101 (2002).
[39] A. V. Talyzin and L. S. Dubrovinsky, Phys. Rev. B **68** 233207 (2004).